A NUMERICAL ANALYSIS OF SLOPE FAILURE IN WELDED TUFF CAUSED BY THE IWATE-MIYAGI NAIRIKU EARTHQUAKE IN 2008

Yuichi Nakashima[1*], Senro Kuraoka[2], Yoshiya Hata[3]

ABSTRACT

In this research the mechanism of rock slope failure was studied through filed investigation, laboratory strength tests, and numerical analyses. The result of the field investigation and laboratory tests, suggested that the oscillating behavior of the jointed rock slope may have been markedly amplified due to the fact that the upper part of slope was composed of hard welded tuff with high density underlain by soft pumice tuff with low density. Dynamic simulation of the jointed rock slope was performed, with the distinct element method in order to examine this hypothesis. The results of the numerical analyses indicate that stiffness of the jointed rock have significant bearings on the stability of rock slope subjected to seismic loads.

Key Words: Earthquakes, Slope failure, Distinct element method

INTRODUCTION

Iwate-Miyagi Nairiku Earthquake in June, 2008, caused a large number of sediment disasters such as the landslide, slope failure, and debris flow. Ministry of Land Infrastructure Transport and Tourism reported that 80 percent of the 23 missing or dead person, caused by the earthquake, was due to sediment disasters, suggesting that most of the critical losses were induced by the sediment disasters. Moreover, massive slope failures facing rivers have formed 15 natural landslide dams which posed potential risks of dam breaks.

In this research a particular interest is placed on the mechanisms of numerous rock slope failures found along the road and rivers. Investigation conducted by academic societies, government agencies, and consulting firms found many rock slope failures, exhibiting a unique feature, in that the upper layer consisted of rigid welded tuff with distinct vertical joints, whereas the lower layer consisted of soft tuff with few joints.

FIELD INVESTIGATION

Fig.1 shows the location of investigation. Photographs 1 and 2 show the slope failure at the site A and the site B, respectively. At the site A, the slope failure occurred due to the

1 Engineer, River Basin & Urban Infrastructure Div. Geology & Geotechnology Dept., Nippon Koei Co., LTD., 2, Kojimachi 4-chome, Chiyoda-ku, Tokyo, JAPAN (*Corresponding Author; tel:+81-3-3238-8355; Fax: ++81-3-3238-8230; Email: a5801@n-koei.co.jp)
2 Dupity Manager, Research and Development Center, Nippon Koei Co., LTD., 2304, Inarihara, Tsukuba-shi, Ibaraki, JAPAN
3 Researcher, Research and Development Center, Nippon Koei Co., LTD., 2304, Inarihara, Tsukuba-shi, Ibaraki, JAPAN

earthquake. The dimensions of slope failure are about 120 m in height and about 250m in width. The upper part of the slope consists of stiff welded tuff with well-developed columnar joints and lower part consists of soft pumice tuff. The collapsed rock masses were near the geologic boundary and the river indicated as Sanhazama River in Fig. 1. A Similar geological structure was discovered at the site B. In both cases, the rock mass has reached the opposite bank of the river.

Photograph 3 shows the outcrop near the site B. Photographs 4 and 5, show the steel wedge that was hammered in to the two types of rocks, in order to illustrate difference in the stiffness and strengths of the welded tuff and pumice tuff. These photographs show that the wedge could not be hammered in to the welded tuff for more than 1 cm, whereas the wedge could be easily hammered into the pumice tuff for more than 5 cm. The differences in the mechanical properties of welded tuff and pumice tuff were examined by uniaxial compression and ultrasonic tests of samples obtained from the site B.

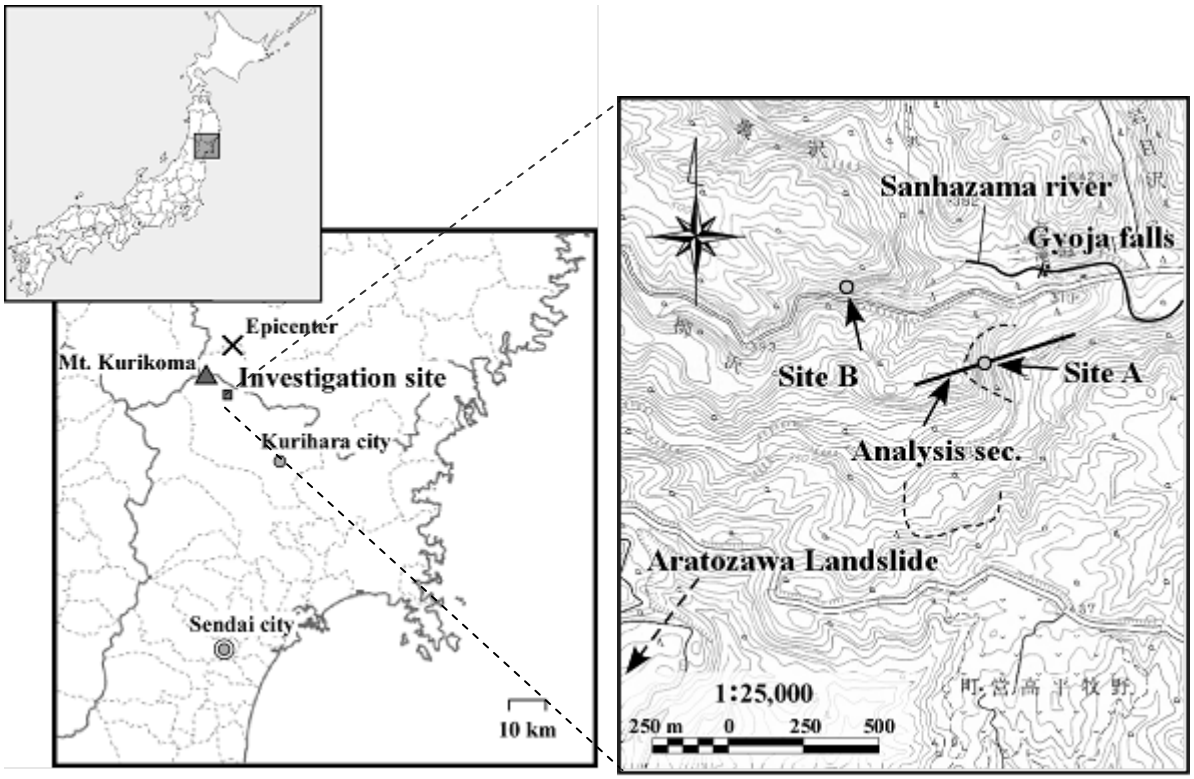

Fig.1 The location of investigation

Photograph 1 Slope failure at the site A

Photograph 2 Slope failure at the site B

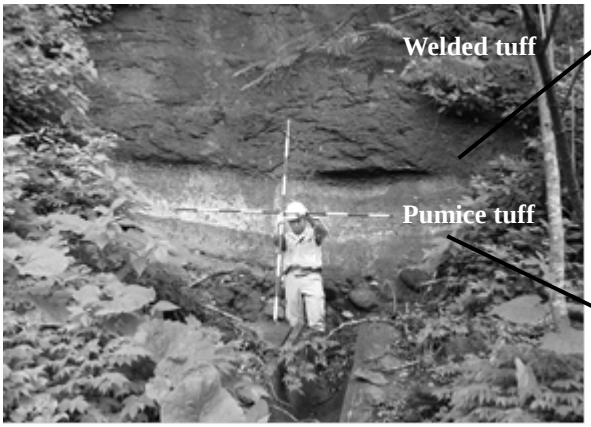

Photograph 3 Outcrop nearby the site B

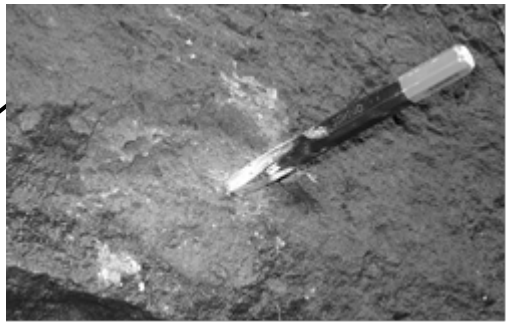

Photograph 4 Welded tuff. The wedge penetrated less than 1 cm

Photograph 5 Pumice tuff. The wedge penetrated more than 5 cm

LABORATORY TEST

Laboratory tests results are shown in table.1. These laboratory tests result shows that the deformation property and the strength property in upper part of the slope are greatly different from those of lower part of the slope. Young's modulus (E) of welded tuff obtained from uniaxial compression test was 4.3×10^4 MPa, and it was much higher than that of pumice tuff. Dynamic elastic modulus (Ed) obtained from ultrasonic velocity measurement test showed similar trends. Compressive strength of welded tuff was 96.2 MPa, and it was also higher than that of pumice tuff.

The result of the field investigation and laboratory tests, suggested that the oscillating behavior of the jointed rock slope may have been markedly amplified due to the fact that the upper part of slope was composed of hard welded tuff with high density underlain by soft pumice tuff with low density.

Dynamic simulation of the jointed rock slope was performed, with the distinct element method in order to examine this hypothesis.

Table 1 Laboratory tests results

		Welded Tuff	Tuff	Pumice tuff
	Unit weight γ (kN/m^3)	26.7	21.7	15.7
Ultrasonic wave test	Longitudinal wave Vp (km/sec)	4.71	2.58	1.41
	Transversal wave Vs (km/sec)	2.19	1.43	0.63
	Poisson's ratio ν_d	0.36	0.28	0.38
	Dynamic modulus of elasticity E_d (MPa)	3.6×10^4	1.2×10^4	1.9×10^3
Unconfined compression test	Unconfined compression strength σ_c (MPa)	96.7	14.6	2.3
	Secant modulus of elasticity E_s (MPa)	4.3×10^4	5.9×10^3	3.3×10^2

NUMERICAL ANALYSIS OF SLOPE FAILURE

Analysis model

Fig.2 shows the distinct element method (DEM) model for the dynamic simulation. In case of jointed rock masses, DEM is based on discontinuum approach and is therefore suitable to simulate behaviors exhibiting large movements such as rockfall.

There is no detailed profile of the slope, and the similar slope failure was discovered in several sites. Hence, the simplified model was made for the dynamic simulation based on the simple measurement using handy laser distance meter.

The model consists of the following three layers: welded tuff, pumice tuff, and tuff. The columnar joints were generated in the front region of the welded tuff. On bottom and both sides of DEM analysis model, boundary conditions are as follows:

Bottom: Vertical: fixed boundary, Horizontal: viscous boundary
Side: Vertical: fixed boundary, Horizontal: viscous boundary with free field

All the rock mass were modeled as elastic model. In the analysis, physical properties of rock mass were determined from laboratory tests. The joint strength parameters were used typical small value given in Table 2. A Rayleigh damping was used to get more reliable results.

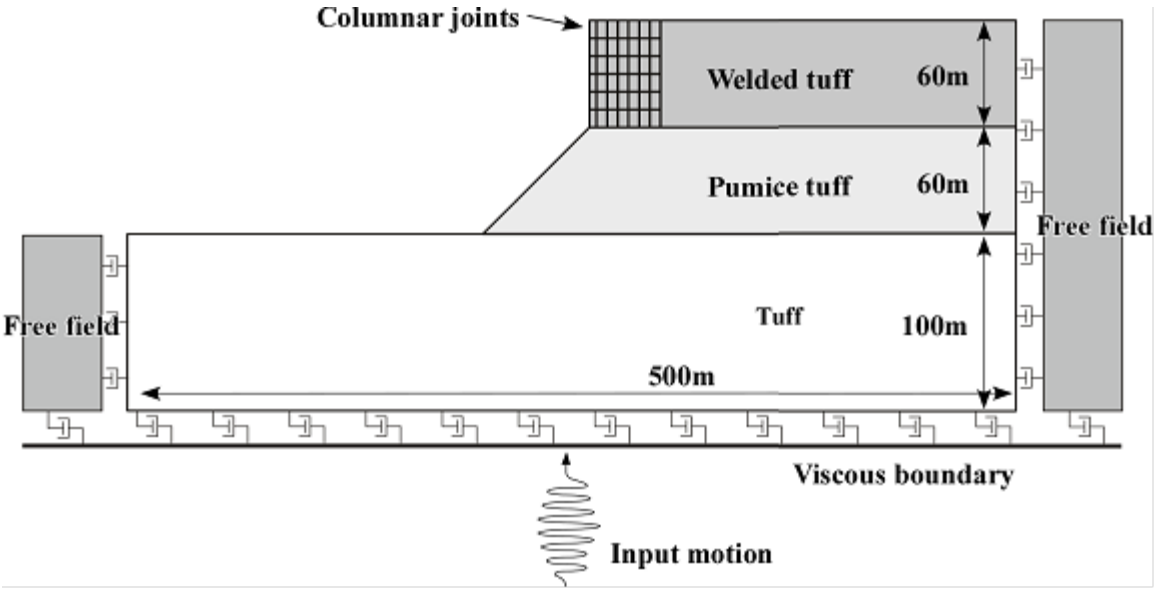

Fig. 2 DEM model for the dynamic simulation

Table 2 Physical properties of rock mass and joints

	Unit weight γ (kN/m^3)	Modulus of Elasticity E (MPa)	Poisson's ratio ν	Cohesion c (kPa)	Internal friction angle ϕ (degree)	Tensile strength σ_t (kPa)
Welded Tuff	26.7	4.3×10^4	0.36	-	-	-
Pumice Tuff	15.7	3.3×10^2	0.38	-	-	-
Tuff	21.7	5.9×10^3	0.28	-	-	-
Columnar joints	-	-	-	10	20	1

Input motion

There is no station that has recorded the strong motion near the targeted site. Hence, in this study, strong earthquake motion in the site was estimated using the stochastically simulated Green's function method (Kamae *et al.*, 1991). The characterized source model for strong ground motion was generated by the waveforms inversion method (Nozu, 2008; Hata *et al.*, 2009) that is based on the seismic slip distribution. The ground shaking characteristics in the site was based on the subsurface structural model by the National Research Institute for Earth Science and Disaster Prevention (NIED). The theoretical waveform by numerical calculation of strong ground motion was adopted as input earthquake motion for the DEM model.

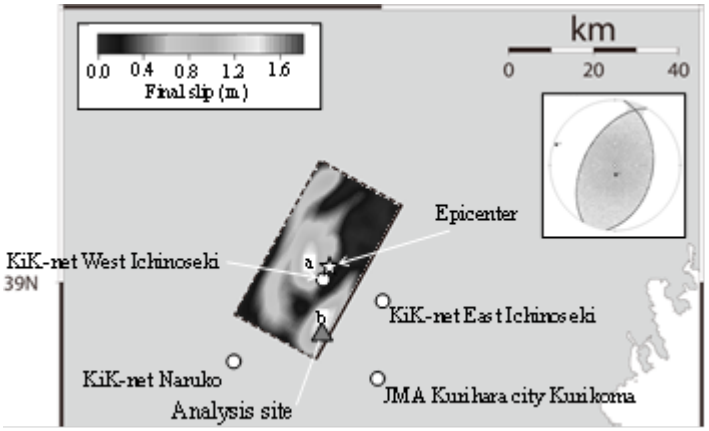

Fig. 3 The characterized source model for strong ground motion prediction

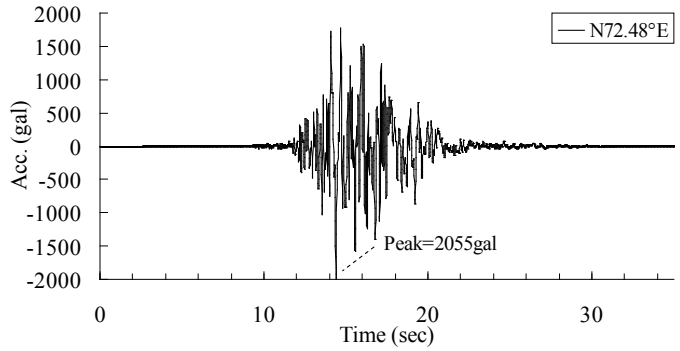

Fig. 4 Input earthquake motion (2E; the rock outcrop motion) by numerical calculation of strong ground motion

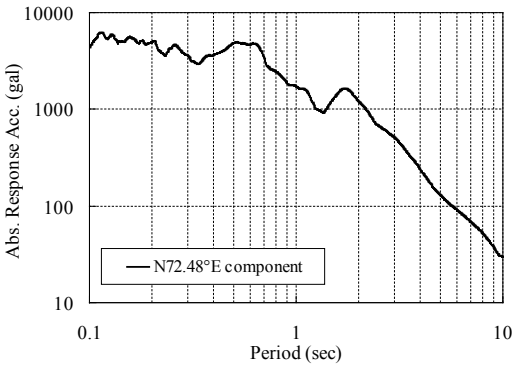

Fig. 5 Absolute response acceleration of input earthquake motion

Analysis cases

Table 3 shows the analysis cases. In case 1, we set the actual geological structure. Other cases were conducted in order to study the influence of the difference in geological structure upon slope failure. In case 2, we hypothesized that both upper and lower part of slope were composed of hard welded tuff. In case 3, we hypothesized that both upper and lower part of slope were composed of soft pumice tuff.

Table 3 Analysis cases

	Case 1 **Actual geological structure**	**Case 2** **Hypothetical case**	**Case 3** **Hypothetical case**
Upper part	Welded tuff (hard)	Welded tuff (hard)	Pumice tuff (soft)
Lower part	Pumice tuff (soft)	Welded tuff (hard)	Pumice tuff (soft)
Bedrock	Tuff	Tuff	Tuff

Basic dynamic property

In order to study the basic dynamic property of slope, eigenvalue analysis and frequency response analysis were conducted, using FEM model without joints.

Table 4 shows results of eigenvalue analysis. Fig. 6 shows result of frequency response analysis. Predominant period of case 1 (actual geological structure) appear at 0.4 seconds, 1.0 seconds, and 2.0 seconds. On the other hand, predominant period of case 2 is shorter than 0.4 seconds. Predominant period of case 3 appear at similar period of the case 1. It is assumed that the slope response is amplified at 2.0 seconds therefore, due to the soft pumice tuff.

Table 4 Results of eigenvalue analysis

Mode	**Frequency (Hz)**	**Period (sec)**	**Modal participation factor**		**Effective mass ratio**	
			X	**Y**	**X**	**Y**
1	0.504	1.986	251.1	9.9	0.373	0.001
2	1.059	0.945	17.9	-217.6	0.002	0.287
3	2.036	0.491	187.3	19.2	0.207	0.002
4	2.265	0.441	-71.3	-18.5	0.030	0.002
5	2.634	0.380	114.0	-91.3	0.077	0.051
6	2.764	0.362	187.1	39.6	0.207	0.010
7	3.046	0.328	-16.1	-32.8	0.002	0.007
8	3.138	0.319	30.2	-33.3	0.005	0.007

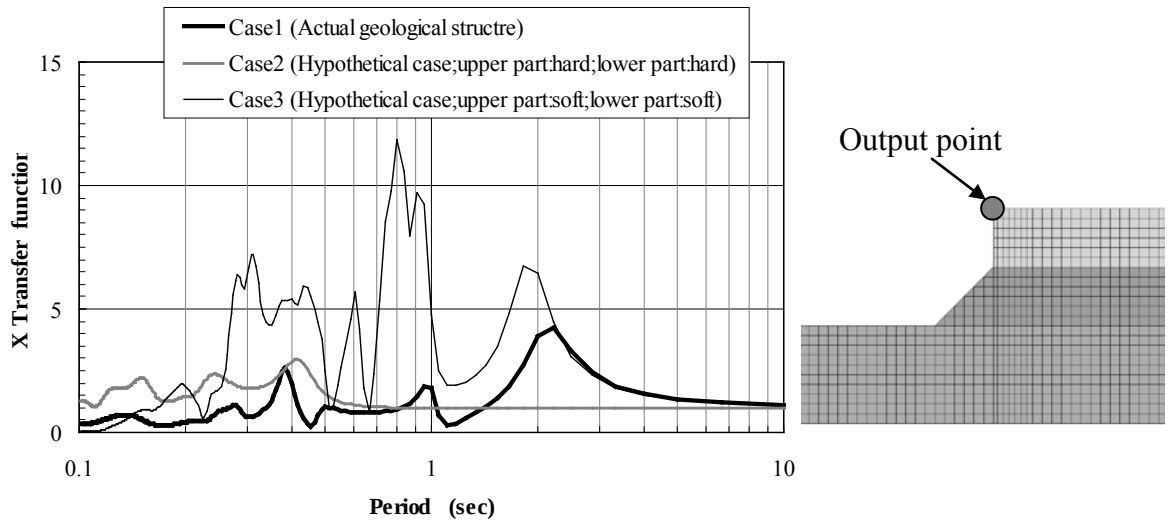

Fig. 6 Result of frequency response analysis

Analysis results

Fig.7 shows DEM analysis results at 20 seconds and 40 seconds. In case 1, the columnar joints clearly opened after 20 seconds and the rock masses started to incline toward the river, followed by toppling failure, where broken rock pieces fell up to the toe of the lower layer. The travel distances of the broken rock pieces were similar in the filed.

In case 2, the columnar joints started to open approximately 20 seconds after the initiation of excitation. However, the jointed rock mass did not fail. In case 3, while the behavior of the rock mass is similar to that of case 1, more rocks have fallen than in case 1.

Fig.8 shows horizontal displacement time history of top of the slope. The maximum displacement was about 1.0 m in case 1 and case 3. By contrast the maximum displacement was about 0.5 m in case 2.

These simulated results, such as the toppling failure and the amplitudes of the displacements, are thought to be consistent with the behaviors that are expected from the observation of the spreads of debris and joint systems. Hence, it is assumed that the slope failure is affected by the existence of soft pumice tuff and the columnar joints.

	Case 1 Actual geological structure Upper part: Welded tuff Lower part: Pumice tuff	Case 2 Hypothetical case Upper part: Welded tuff Lower part: Welded tuff	Case 3 Hypothetical case Upper part: Pumice tuff Lower part: Pumice tuff
20sec	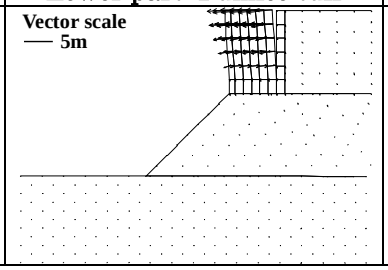	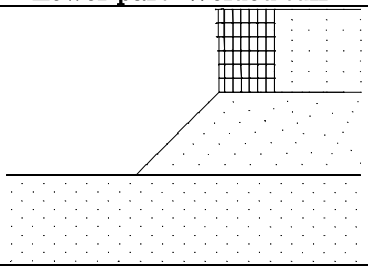	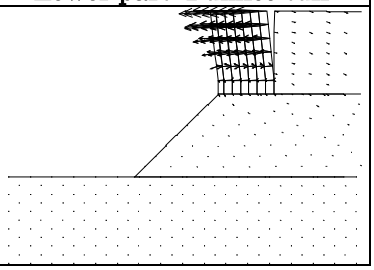

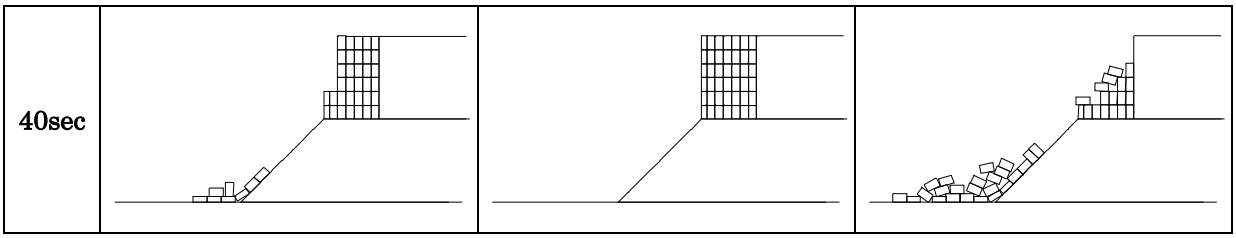

Fig. 7 DEM analysis results at 20 seconds and 40 seconds

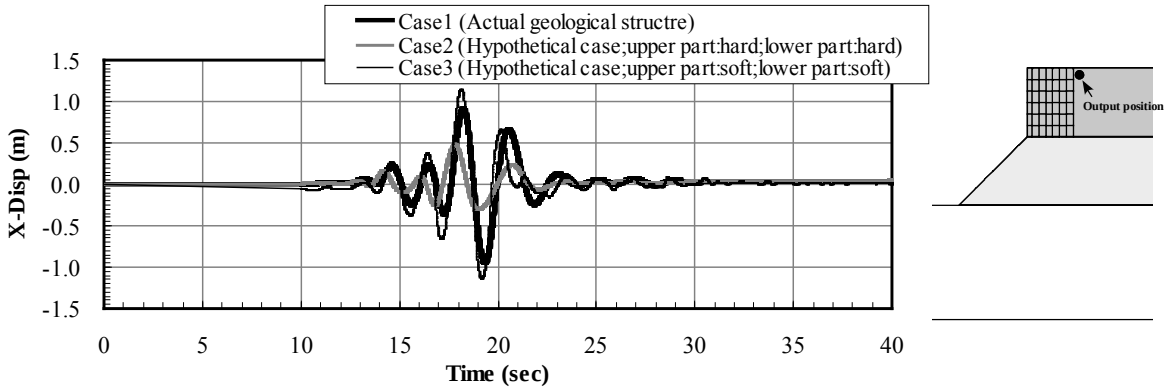

Fig. 8 Horizontal displacement time history of top of the slope

CONCLUSIONS

In this research the mechanism of rock slope failure was studied through field investigation, laboratory tests, and numerical analyses. The findings are described below.

1 The laboratory test results show that the deformation property and the strength property in upper part of the slope are significantly different from those of lower part of the slope.
2 Dynamic simulation results indicated that joint system and the soft pumice tuff are major factors that controlled the slope failure.

The results presented in this paper are at preliminary level and further research is desirable to improve the reliability of the numerical simulation which may be used not only to estimate the travel distance of the rock debris but also to design reinforcements.

REFERENCES

Hata, Y., Osumi, T. and Nozu, A. (2009): *Estimation of the strong motion in the Nuruyu Hot Spring for the 2008 Iwate-Miyagi Nairiku Earthquake based on empirical site amplification and phase effects* (in Japanese), Proc. of the 63rd annual meeting of JSCE (CD-ROM), I-331, pp.661-662.

Kamae, K., Irikura, K. and Fukuchi, Y. (1991): *Prediction of strong ground motion based on scaling law of earthquake by stochastic synthesis method* (in Japanese with English abstract), Jour. of Struct. Constr. Engng, AIJ, No.430, pp.1-9.

Nozu, A (2008): *Source model for the 2008 Iwate-Miyagi Nairiku Earthquake* (in Japanese with English abstract), PARI research note, No.30.